Equilibrium Scour Downstream of Three-Dimensional Grade-Control Structures

S. Michael Scurlock, S.M.ASCE[1]; Christopher I. Thornton, M.ASCE[2]; and Steven R. Abt, F.ASCE[3]

Abstract: To promote grade-control, bank stability, and fish habitat enhancement, three-dimensional structures installed within river channels are becoming increasingly popular choices for rehabilitation. A-, U-, and W-shaped rock weirs are commonly used in streams, yet three-dimensional scour holes develop downstream of the weir crest and often undermine the weir foundation. Current approaches for the prediction of scour depth and geometry are generally extrapolated from the case of two-dimensional flow. Furthermore, data from the literature regarding structures inciting significant lateral flow components are sparse. A series of laboratory experiments were conducted in which data from A-, U-, and W-shaped weirs were collected and evaluated using scour-prediction methodologies, focusing on their applicability to predict maximum scour depths. New dimensionless expressions were developed for the prediction of scour depth downstream of A-, U-, and W-shaped weirs on the basis of laboratory data that incorporate specific parameters accounting for weir geometry. The dimensionless expressions were compared with the most accurate relationship found within the literature, as applied to the compiled database, and mean error was reduced from 37.12 to 10.45%. **DOI: 10.1061/(ASCE)HY.1943-7900.0000493.** © *2012 American Society of Civil Engineers.*

CE Database subject headings: Hydraulic structures; Weirs; Rivers and streams; Scour; Control structures.

Author keywords: Hydraulic structures; Weirs; Rivers; Scour; Grade-control structures.

Introduction

In-stream hydraulic structures can provide energy dissipation, increased aquatic habitat, fish passage, grade-control, and bank and bed stabilization through the diversion of conveyance with the river-channel center. Grade-control structures are typically rectangular, abrupt, and perpendicular to the direction of flow. However, three-dimensional (3D) weirs, which extend along a significant length of the channel, are gaining in popularity. The Pacific Northwest region of the U.S. Bureau of Reclamation has implemented such structures in attempt to promote fish habitat and passage, and the Middle Rio Grande River Maintenance Project has used the weirs for bank-stabilization design (Reclamation 2007). Common types of 3D grade-control structures employed are the A-, U-, and W-shaped weirs, which are named for their structural resemblance to letters of the alphabet. Weir installations typically occur with few engineering guidelines and anecdotal experience, and as a result, downstream scour pools often develop that undermine the structure foundation.

Hoffmans and Pilarczyk (1995) describe the clear-water scour process with an initial phase, developmental phase, stabilization phase, and equilibrium phase. The initial phase is characterized by the most significant sediment transport from the scour zone and the incipient formation of the scour geometry. During the developmental phase, the characteristic scour shape remains relatively constant, and the upper portion of the upstream slope reaches equilibrium, but scour-depth increases dramatically. Stabilization occurs when the change of scour-depth with time decreases and scour-hole dimensions increase more downstream than vertically. Equilibrium phase is obtained when dimensions of the scour-hole no longer appreciably change with time and a hydraulic balance is achieved within the system.

Bormann (1988) provides a comprehensive explanation of two-dimensional (2D) scour hydraulics and equilibrium balance, incorporating the physics governing scour phenomenon. Fig. 1 depicts a schematic of the 2D scour process in which a plunging jet of initial thickness y_o and velocity u_o travels along path S through the tailwater. Diffusion occurs because of large velocity gradients, and the jet is redirected at a reduced bed velocity u_o^*. When forces about a sediment particle contact point incited by u_o^* exceed forces caused by the submerged particle weight, incipient motion and sediment transport from the scour hole ensue. Bed-material displacement from the scour hole continues until the path of the impinging jet is sufficiently long to allow diffusion such that u_o^* is less than the minimum value required for transport. Such geometry conditions are typically termed as equilibrium; however, small perturbations occur within scour depths related to turbulence from periodic vortex formation (Hopfinger et al. 2004; Gaudio and Marion 2003). Mason and Arumugan (1985) stated that for all practical purposes, variations within equilibrium scour depth are relatively small, and the concept of a maximum scour depth can be accepted, especially when considering engineering design.

A 3D jet observed over the crest of rock weirs exhibits constructive and destructive interference as various jet paths merge and incites larger degrees of turbulence than found in 2D flow. The tolerance of variation for equilibrium scour-depth in a 3D flow is thereby increased from a 2D scenario. Additional turbulence generated by labyrinth weirs, structures with repeated cycles of

[1]Graduate Research Assistant, Dept. of Civil and Environmental Engineering, Engineering Research Center, Colorado State Univ., Fort Collins, CO 80523 (corresponding author). E-mail: scurlock@engr.colostate.edu

[2]Assistant Professor and Director, Engineering Research Center and Hydraulics Laboratory, Dept. of Civil and Environmental Engineering, Colorado State Univ., Fort Collins, CO 80523. E-mail: thornton@engr.colostate.edu

[3]Professor, Dept. of Civil and Environmental Engineering, Colorado State Univ., Fort Collins, CO 80523. E-mail: sabt@engr.colostate.edu

Note. This manuscript was submitted on August 31, 2009; approved on July 22, 2011; published online on July 25, 2011. Discussion period open until July 1, 2012; separate discussions must be submitted for individual papers. This paper is part of the ***Journal of Hydraulic Engineering***, Vol. 138, No. 2, February 1, 2012. ©ASCE, ISSN 0733-9429/2012/2-167–176/$25.00.

trapezoidal or triangular design features similar to rock weirs, is described by Falvey (2003).

Literature regarding the prediction of scour downstream of drop structures is extensive, and the physical process has been under investigation since original work conducted by Schoklitsch (1932). Despite numerous investigations, there does not appear to be a procedure sufficiently robust to describe maximum scour-depth over a wide range of conditions. Furthermore, little information is available in which methodologies have been developed specifically for A and U weir shapes. Bhuiyan et al. (2007) studied a W-shaped weir installed along a model river bend in which they modified results from Bormann and Julien (1991) to coincide with collected data. Bormann and Julien (1991) expanded the relationship of Mason and Arumugam (1985) to incorporate variables within their own research and to summarize equilibrium scour equations from Schoklitsch (1932) to Bormann (1988), in which exponents of the equation are unique to individual studies, expressed as

$$y_{SE} + z_d = K\left(\frac{q^a u_o^b H_T^c y_t^d \beta'^e}{g^f d_s^i}\right) \tag{1}$$

in which a, b, c, d, e, f, and i = exponents dependent on each study; d_s = effective grain diameter; g = gravitational acceleration; H_T = total head drop over structure; K = coefficient dependent on diffusion and bed-material properties; q = unit discharge over structure; u_o = jet velocity over structure; y_{SE} = equilibrium scour depth; y_t = tailwater depth; z_d = drop height; and β' = jet-impingement angle at bed impact (Fig. 1). A comprehensive review of the exponents specific to each study to which Eq. (1) applies can be found in Bormann and Julien (1991). Many of the studies that Eq. (1) encompasses, such as Mason and Arumugan (1985), are limited by their experimental use of uniform grain distributions, as noted by Machado (1987). The form of Eq. (1) is also limited to applications in which scour depth is greater than the structure drop height.

Scour downstream of rectangular structures has been described by dimensional analysis of predictive variables. Gaudio and Marion (2003), expanding work by Gaudio et al. (2000), described downstream equilibrium scour for uniform grain-size distributions by performing least-squares linear regression on identified predictive variables as

$$\frac{y_{SE}}{H_S} = 0.180\left[\frac{A_1}{(\Delta - 1)d_{50}}\right] + 0.369 \tag{2}$$

in which A_1 = morphological jump, defined as the difference between initial and final slope multiplied by the length between structures; d_{50} = mean sediment diameter; H_S = critical specific energy over structure; and Δ = specific gravity of material. Similar dimensional-analysis methodologies incorporating similar parameters as Eq. (2) include Meftah and Mossa (2006) and Lenzi et al. (2002).

D'Agostino and Ferro (2004) proposed that scour downstream of grade-control structures in alluvial channels can be represented by the following functional relationship:

$$f(y_{SE}, z, b, B, y_t, H, Q, \rho_S, \rho, g, d_{50}, d_{90}) = 0 \tag{3}$$

in which b = weir width; B = channel width; d_{90} = sediment diameter in which 90% total is smaller by size; H = piezometric drop across structure; Q = discharge; z = fall height; ρ = fluid density; and ρ_S = sediment density.

Applying incomplete self-similarity theory to the variables in Eq. (3), accompanied by a multiple regression of the logarithms using data from Veronese (1937), Bormann and Julien (1991), D'Agostino (1994), Mossa (1998), and D'Agostino and Ferro (2004), produced the following:

$$\frac{y_{SE}}{z} = 0.540\left(\frac{b}{z}\right)^{0.593}\left(\frac{y_t}{H}\right)^{-0.126}\left[\frac{Q}{bz\sqrt{g(\Delta-1)d_{50}}}\right]^{0.544} \times \left(\frac{d_{90}}{d_{50}}\right)^{-0.856}\left(\frac{b}{B}\right)^{-0.751} \tag{4}$$

In a similar methodology as D'Agostino and Ferro (2004), Comiti et al. (2006) produced a relationship for scour depth

$$\frac{y_{SE}}{z} = 2.00\left(\frac{H_S}{z}\right)^{0.590}\left(\frac{b}{B}\right)^{2.34}\left(\frac{\Delta d_{90}}{z}\right)^{-0.09} \tag{5}$$

Eqs. (4) and (5) deviate from those previously presented as they account for nonuniform sediment gradations and channel geometry. Structure geometry parameters represented within these expressions are not included in other dimensional-analysis predictive methodologies and the dimensionless b/B term provides consideration for 3D flows owing to channel contractions. However, the equations are limited in applicability to 3D grade-control. Data used for regression analyses were collected from weirs installed normal to the thalweg axis, and lateral flows from channel contractions that b/B may account for are relatively negligible compared with lateral flows observed through A-, U-, and W-shaped weirs. Definitions of necessary parameters for calculation in the preceding equations, such as weir length and fall height, are ambiguous for 3D structures, as these parameters vary with channel length. Furthermore, critical energy at the sill is a complex parameter to determine for 3D grade-control structures because its location cannot be demarcated by a classical one-dimensional channel cross-section. Fig. 2 shows a downstream view of critical flow and associated hydraulic jump through a U-shaped weir installed in a laboratory setting.

Equation development for equilibrium jet scour holes downstream of hydraulic structures grounded in more theoretical means has been addressed by numerous authors. Fahlbusch (1994), Hoffmans and Pilarczyk (1995), and Hoffmans (1998) introduce predictive methodologies on the basis of 2D force balances with empirical coefficients accounting for turbulent kinetic energy near the bed. However, the assumption of angle symmetry surrounding the location of maximum scour was determined invalid for rock-weir scour.

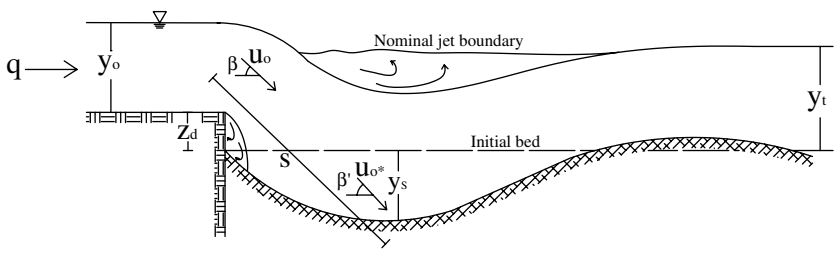

Fig. 1. Schematic of flow through two-dimensional grade-control scour (adapted from Bormann 1988)

J. Hydraul. Eng. 2012.138:167-176.

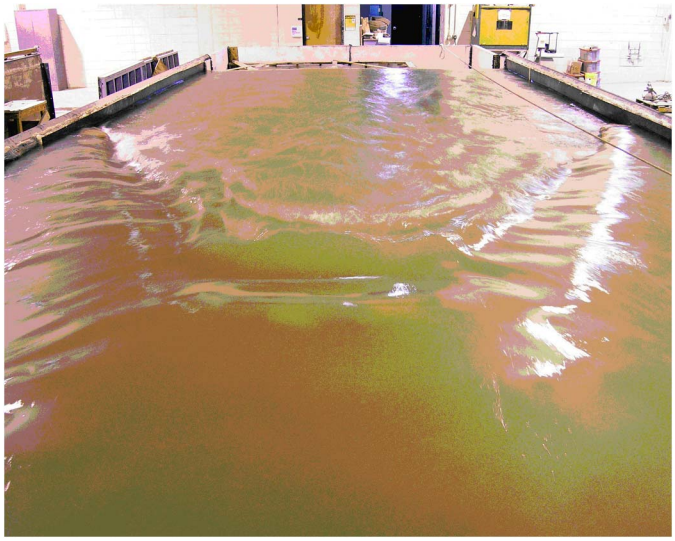

Fig. 2. Critical flow over a U-shaped weir crest (image courtesy of CSU/USBR)

Most approaches found in the literature that approximate maximum equilibrium scour depth were developed for the case of 2D flow, incorporating parameters not applicable to 3D grade-control. Parameters include cross-section definitions of critical energy, structure width, fall height, bed geometry, and jet geometry. The objectives of this study are to (1) develop a dimensional-analysis–based predictive methodology, accounting for structure geometry, that will predict the maximum scour-depth pertaining to 3D weir shapes; (2) conduct a flume study using A-, U-, and W-shaped weir shapes to measure the maximum scour-depth downstream of these structures from a range of flow conditions; and (3) calibrate predictive methodologies to laboratory data using regression analysis.

Laboratory Experiments

A hydraulic testing program was conducted by Scurlock (2009) at the Colorado State University Engineering Research Center Hydraulics Laboratory to evaluate scour downstream of 3D A-, U-, and W-grade-control structures. A series of 27 experiments was performed in a flume 4.88-m wide, 15.24-m long, and 1.22-m deep (Fig. 3).

The flume comprises an intake manifold, flow baffle, head box/transition section, test section incorporating the weir structures, outlet section with tailwater control, and tail box. Granular bed material was placed throughout the flume extending from the entrance of the test section to the tailwater control. The data collected during each test included discharge, water surface elevation, flow depth, flow velocity, and scour depth. A movable cart spanned the width of the flume, which facilitated data collection. A measuring tape of ± 0.003-m accuracy was placed along the cart and flume walls for positioning. A 75-horsepower (hp) centrifugal pump and a 40-hp centrifugal pump were used to deliver flows from the laboratory sump to the flume head box. Flows from the 75-hp pump were regulated with an orifice plate, with an associated accuracy of approximately $\pm 2.5\%$ of the total measured flow rate; flows from the 40-hp pump were measured with an Endress + Hauser PROline Promag 53 electromagnetic flow meter, with an approximate accuracy of $\pm 0.5\%$.

Modeled A-, U-, and W-shaped weir structures were designed using Bureau of Reclamation (2007) criteria and constructed at the largest size possible given flume constraints. Bed-material sizing was 15, 9.8, and 5 mm. Sediment gradations were obtained from sieve analysis of the materials. A specific gravity value of 2.65 was used for all materials. Small cobbles were representative of the Pacific Northwest region, and coarse gravel was selected as representative material of Rio Grande headwater streams. If the model weirs were scaled to identified prototype locations, a Froude scale of 1:5.75 applies for the Pacific Northwest region and 1:4.36

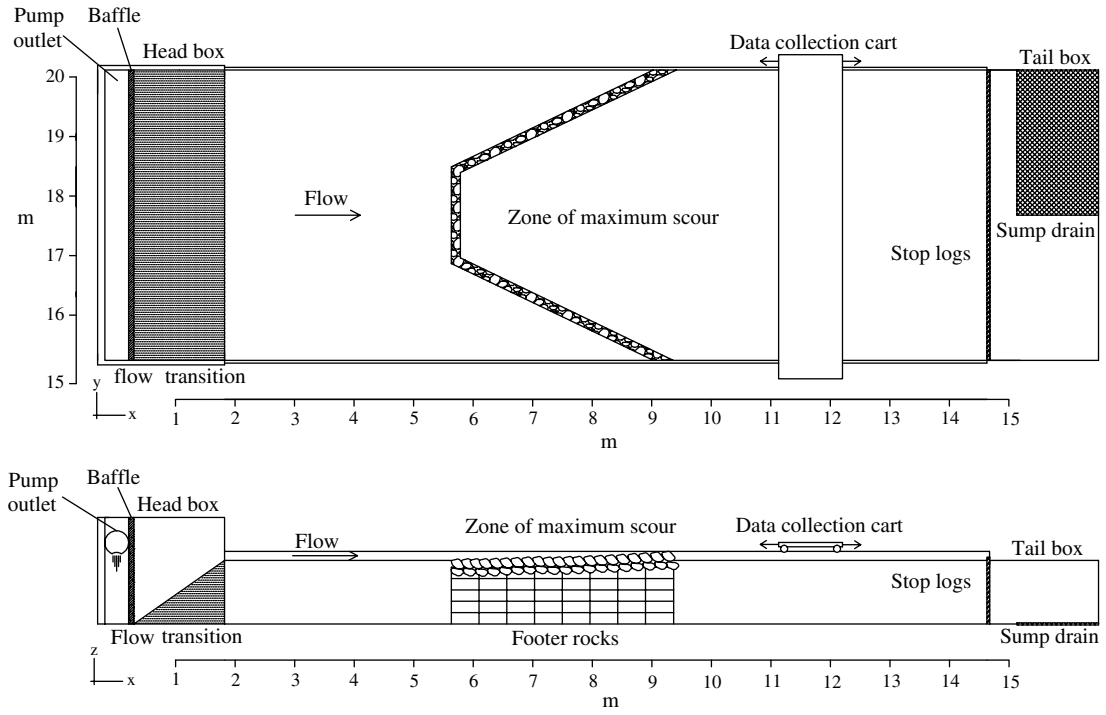

Fig. 3. Flume schematic

J. Hydraul. Eng. 2012.138:167-176.

for the upper Rio Grande; however, modeled weirs are not restricted in scaling to other prototype scenarios.

Independent variables tested for each weir shape included discharge, weir arm length, weir plan and weir profile angles, weir drop height, weir rock size, bed-material size and gradation, and bed slope. All weir configurations were designed to be evaluated at an increasing sequence of one-third bank-full, two-thirds bank-full, and bank-full discharges. The upstream apex of each weir was constructed near station 5.5. Weirs were constructed with an anchor wall, foundation footer rock, and header or sill rock (Fig. 4). Anchor walls comprise concrete blocks extending from the flume floor to the foundation rock footer. The rock footer was grouted to the anchor wall immediately atop the blocks. To provide additional energy dissipation, the header rock was grouted to the top of the rock footer, but offset approximately one-third of the rock diameter upstream (Reclamation 2007). Weirs were grouted for structural stability and prevention of interstitial flow through the crest.

After construction of a specified configuration (Cfg), testing procedures were initiated. The bed was surveyed with a point-gauge of ± 0.0003-m accuracy and/or a Leica Scan Station light detection and ranging system. Flow was then initiated, and the model was allowed to run at the specified discharge. The channel bed was not reset between increases in discharge. Time requirements for the testing of equilibrium scour conditions, as reported from the literature, vary from 1 h to multiple days. For the current research, baseline testing was conducted on a W-shaped weir to determine an appropriate duration for equilibrium conditions to develop by monitoring sediment transport over time. Twelve hours was determined as a reasonable duration to establish equilibrium geometry. Stop logs were placed at the downstream end of the flume to adjust the tailwater to normal depth within the flume.

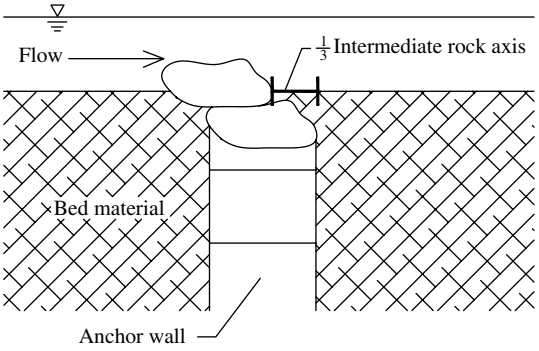

Fig. 4. Footer rock schematic

Once the scour hole attained a state of equilibrium, a side-facing 25-Hz acoustic Doppler velocimeter (ADV) was used to collect 3D velocity data at 20, 60, and 80% of the flow depth within the flume. The accuracy of the device was $\pm 1\%$ of the total magnitude of the measured velocity. Velocity and temperature measurements were taken at 30-s sampling periods at positions shown in Fig. 5. Temperatures were recorded from the ADV to an accuracy of ± 0.01°F. Data were analyzed and despiked using WinADV software and the 60% depth values used for analysis fell within the acceptable range for high-quality data when the signal-to-noise ratio and correlation values were examined, as defined by Bhuiyan et al. (2007).

After the collection of velocity data, the flume was drained, and topographic data were collected. It was assumed that draining the flume for the collection of topographic data would have minimal effects on settling of bed materials or reshaping of the scour geometry. This assumption was validated as surveyed scour-hole geometries exhibited slopes substantially less than the angle of repose for the bed material defined by Simons (1957), such that sloughing and scour-hole refill were considered minimal at the termination of discharge. Topographic surfaces were interpolated and compared with baseline conditions to ascertain scour areas and depths throughout the flume. Displaced bed-material volume was determined as the amount of material moved from within a delineated scour-hole boundary, thereby neglecting general sedimentation patterns within the flume. Maximum scour depths were determined from point-gauge measurements for consistency.

Scour-Depth Dimensional Analysis

Dimensional-Analysis Predictive Methodology Development

The compiled dataset for the A-, U-, and W-shaped weirs is shown in Table 1 and includes equilibrium scour depth and displaced volume of bed material at equilibrium. The areas of scour were mapped after each test (Fig. 6). A- and U-shaped weir scour geometries were observed to be relatively homogeneous across tests with a longitudinally symmetric scour hole forming along the channel centerline. W-shaped weirs produced variable scour patterns across tests that were not found to be longitudinally symmetrical. All weir shapes produced increased areas of sediment transport at the intersection of weir arms. Scour depth at equilibrium conditions within

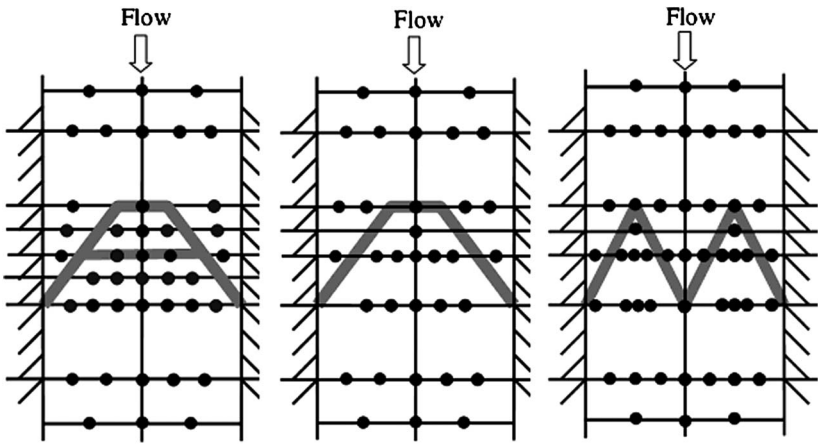

Fig. 5. Velocity collection locations

J. Hydraul. Eng. 2012.138:167-176.

Table 1. Test Matrix, Collected Data, and Predicted Scour Depths

Shape/Cfg/Test	$y_{SE\text{-}obs}$	$y_{SE\text{-}pred}$	V	Q	L_A	z_d	d_{50}	d_{90}	H	θ	ζ	η	b_i	z_i	S_o
—	m	m	m^3	m^3/s	m	m	mm	mm	m	rad	rad	rad	m	m	—
U/a/1	0.10	0.08	0.12	0.283	2.996	0.052	9.80	15.876	0.073	0.497	0.044	—	8.450	0.102	0.0033
U/a/2	0.13	0.11	0.315	0.566	2.996	0.052	9.80	15.876	0.073	0.497	0.044	—	8.450	0.102	0.0033
U/a/3	0.12	0.14	0.377	0.85	2.996	0.052	9.80	15.876	0.039	0.497	0.044	—	8.450	0.102	0.0033
U/b/1	0.32	0.34	0.473	0.184	3.426	0.055	4.20	7.880	0.080	0.443	0.03	—	9.213	0.092	0.0021
U/b/2	0.54	0.48	1.611	0.377	3.426	0.055	4.20	7.880	0.081	0.443	0.03	—	9.213	0.092	0.0021
U/b/3	0.48	0.59	1.969	0.566	3.426	0.055	4.20	7.880	0.052	0.443	0.03	—	9.213	0.092	0.0021
A/a/1	0.16	0.15	0.165	0.184	2.816	0.110	4.20	7.880	0.096	0.523	0.018	—	6.504	0.088	0.0021
A/a/2	0.28	0.29	0.932	0.377	2.816	0.110	4.20	7.880	0.090	0.523	0.018	—	6.504	0.088	0.0021
A/a/3	0.41	0.41	1.979	0.566	2.816	0.110	4.20	7.880	0.081	0.523	0.018	—	6.504	0.088	0.0021
W/a/1	0.22	0.19	0.125	0.184	2.429	0.055	4.20	7.880	0.065	0.465	0.041	0.011	10.877	0.090	0.0021
W/a/2	0.45	0.35	1.264	0.377	2.429	0.055	4.20	7.880	0.065	0.465	0.041	0.011	10.877	0.090	0.0021
W/a/3	0.41	0.49	1.635	0.566	2.429	0.055	4.20	7.880	0.041	0.465	0.041	0.011	10.877	0.090	0.0021
U/c/1	0.10	0.10	0.156	0.283	3.834	0.052	9.79	17.277	0.095	0.401	0.036	—	9.960	0.102	0.0033
U/c/2	0.14	0.15	0.791	0.566	3.834	0.052	9.79	17.277	0.085	0.401	0.036	—	9.960	0.102	0.0033
U/c/3	0.24	0.18	1.642	0.85	3.834	0.052	9.79	17.277	0.064	0.401	0.036	—	9.960	0.102	0.0033
A/b/1	0.12	0.13	0.277	0.283	2.868	0.104	9.79	17.277	0.137	0.516	0.03	—	6.549	0.093	0.0033
A/b/2	0.24	0.24	1.045	0.566	2.868	0.104	9.79	17.277	0.127	0.516	0.03	—	6.549	0.093	0.0033
A/b/3	0.36	0.34	2.536	0.85	2.868	0.104	9.79	17.277	0.115	0.516	0.03	—	6.549	0.093	0.0033
W/b/1	0.13	0.15	0.193	0.283	2.85	0.052	9.79	17.277	0.085	0.404	0.048	0.016	12.413	0.101	0.0033
W/b/2	0.23	0.26	0.602	0.566	2.85	0.052	9.79	17.277	0.072	0.404	0.048	0.016	12.413	0.101	0.0033
W/b/3	0.32	0.36	0.98	0.85	2.85	0.052	9.79	17.277	0.056	0.404	0.048	0.016	12.413	0.101	0.0033
A/c/1	0.16	0.16	0.207	0.377	3.258	0.085	15.38	22.063	0.138	0.463	0.042	—	6.896	0.095	0.0047
A/c/2	0.34	0.30	1.651	0.753	3.258	0.085	15.38	22.063	0.131	0.463	0.042	—	6.896	0.095	0.0047
A/c/3	0.40	0.43	2.272	1.133	3.258	0.085	15.38	22.063	0.103	0.463	0.042	—	6.896	0.095	0.0047
W/c/1	0.11	0.12	0.089	0.377	3.353	0.043	15.38	22.063	0.101	0.349	0.055	0.021	14.283	0.110	0.0047
W/c/2	0.23	0.21	1.289	0.753	3.353	0.043	15.38	22.063	0.074	0.349	0.055	0.021	14.283	0.110	0.0047
W/c/3	0.35	0.30	1.842	1.133	3.353	0.043	15.38	22.063	0.058	0.349	0.055	0.021	14.283	0.110	0.0047

the model was compared with predicted values from approaches found in the literature. Table 2 shows cumulative square error for each weir shape, mean percent error, and square correlation coefficient for various methodologies ranked by cumulative square error.

Considering the limitations of applicability of 2D scour equations from the literature to rock weirs, examination of approaches to alter existing, verified equation formats to represent rock-weir structures, jet characteristics, and scour geometries was undertaken. After multiple approaches were considered, it was found that findings reported by D'Agostino and Ferro (2004) best represented parameters manipulated during the test matrix, incorporated parameters readily available from field data, and predicted equilibrium scour depth well when certain modifications were introduced. Modifications to Eq. (4) included expressing the effective weir length and weir height as functions of the channel width B, plan angle θ, outer arm plan angle ζ, and inner arm angle for the W-shaped weir η. Fig. 7 shows profile and plan view angles for each weir and descriptions of weir geometry related to bank-full width. An average of the weir height extending across the channel width emulated the flow contacting the weir at a single location, rather than along the length of the channel. Effective weir length was defined as the total length taken along the weir crest. The upstream weir segment of A-shaped weir geometries was neglected, and the effective length and height were calculated from the downstream crest and arms only. The upstream portion of the structure was excluded from determination of the effective length because the main scouring forces, attributed to jet impingement and vortex formation, were generated downstream of the excluded crest.

Further alteration of Eq. (4) was found to be beneficial in the prediction of equilibrium scour depth for 3D weirs. The densimetric particle Froude number, $Fr^* = Q/\{bz[g(\Delta - 1)d_{50}]^{1/2}\}$, was modified to include the d_{90} grain diameter instead of d_{50}. Schoklitsch (1932), Jaeger (1939), and Eggenberger (1943) use d_{90} instead of d_{50} because of the presence of larger material within the scour hole that forms an armor layer in the equilibrium state. Because normal depth was chosen as the tailwater depth for each configuration and discharge, Eq. (4) was modified to incorporate channel slope and material roughness through the Manning equation and Strickler's relationship. The piezometric head difference was calculated as the change in the average water surface, approximately 0.5 channel widths upstream of the weir crest to the average water surface 1.5 widths downstream of the crest. Substituting these changes into Eq. (4) yields

$$\frac{y_{SE}}{z_i} = a_1 \left(\frac{b_i}{z_i}\right)^{a_2} \left(\frac{y_t}{H}\right)^{a_3} \left[\frac{Q}{b_i z_i \sqrt{g(\Delta - 1)d_{90}}}\right]^{a_4} \left(\frac{d_{90}}{d_{50}}\right)^{a_5} \left(\frac{b_i}{B}\right)^{a_6} \quad i = \{A, U, W\} \tag{6}$$

in which a_1–a_6 = regression coefficients; b_i = effective weir length; and z_i = mean weir height above bed.

Dimensional-Analysis Methodology Results

Multivariate, backward linear regression was performed on the natural logarithms of the terms in Eq. (6), generating a_1–a_6

J. Hydraul. Eng. 2012.138:167-176.

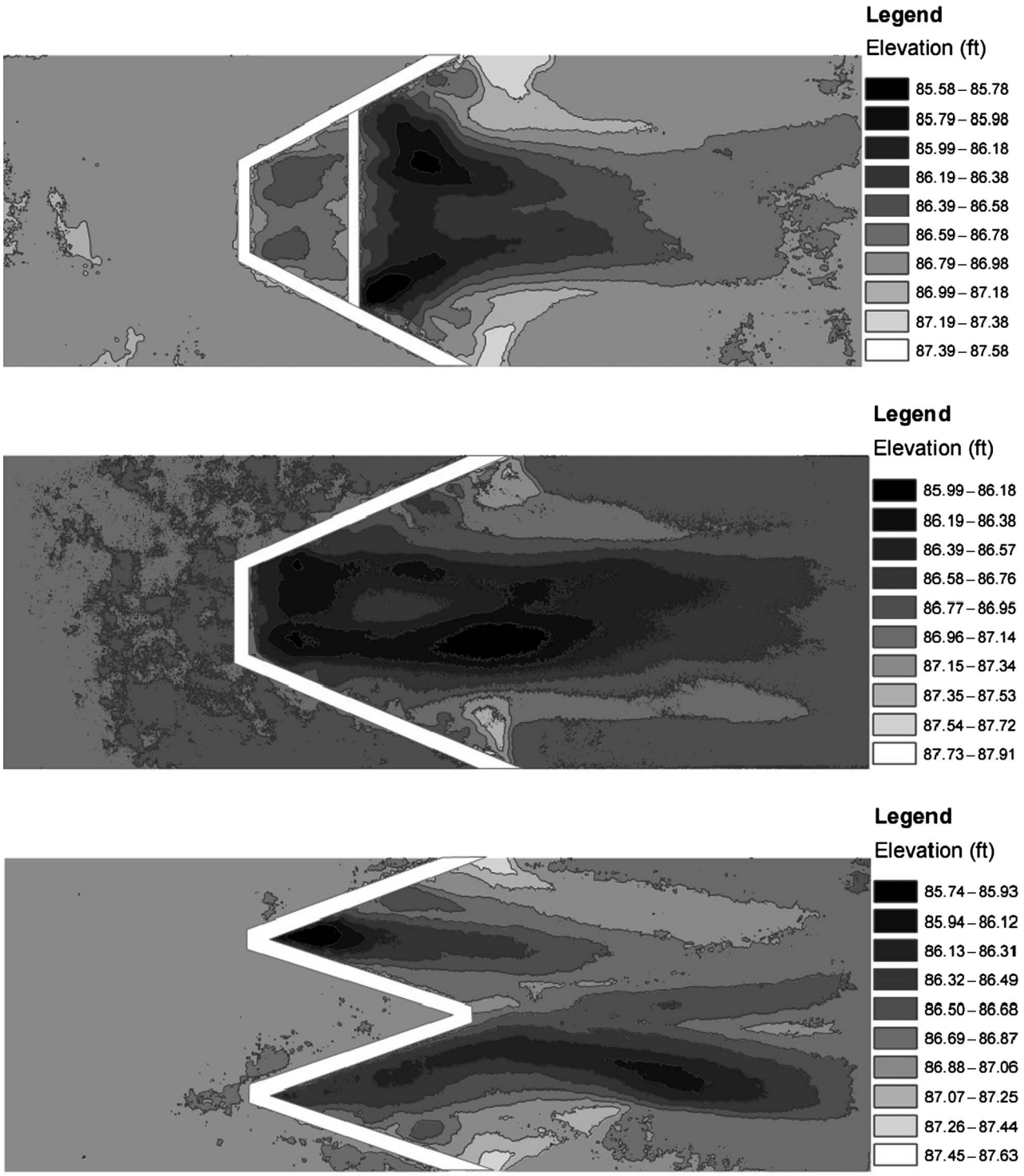

Fig. 6. Representative scour geometries for A-, U-, and W-shaped weirs

regression coefficients for the A-, U-, and W-shaped weirs. Terms not significant at a 0.05 level were eliminated. For the U-shaped weir analysis, the parameter d_{90}/d_{50} was determined to be significant with a large, positive exponent of 9.633. Intuition of the hydraulics governing sediment transport leads to the conclusion that this exponent should be negative, such that an increase in d_{90} with a fixed d_{50} would limit scour potential, coinciding with results from D'Agostino and Ferro (2004), Schoklitsch (1932), Jaegar (1939), and others. This fact, coupled with a small range of d_{90}/d_{50} values evaluated in the laboratory, led to the removal of the term from the U-shaped weir regression analysis.

Results for determining maximum equilibrium scour depth downstream of A-, U-, and W-shaped weirs are respectively given as

$$\ln\left(\frac{y_{SE}}{z_A}\right) = -16.905 + 4.078\ln\left(\frac{b_A}{z_A}\right) + 0.888\ln\left[\frac{Q}{b_A z_A\sqrt{g(\Delta-1)d_{90}}}\right] \quad (7)$$

J. Hydraul. Eng. 2012.138:167-176.

Table 2. Cumulative Square Error (m^2), Mean Error (%), Predicted to Laboratory Data R^2

Source	A-shaped weir	U-shaped weir	W-shaped weir	Total	%	R^2
Schoklitsch (1932)[a]	0.02	0.21	0.07	0.30	37.12	0.35
Qayoum (1960)	0.02	0.21	0.10	0.34	33.57	0.33
Comiti et al. (2006)	0.03	0.25	0.12	0.40	38.00	0.18
Hartung (1959)[a]	0.04	0.27	0.12	0.43	54.56	0.27
Jaegar (1939)[a]	0.08	0.23	0.12	0.43	35.58	0.39
Veronese (1937)[a,b]	0.05	0.29	0.15	0.49	47.10	0.08
Hoffmans (1998)[c]	0.15	0.23	0.15	0.53	38.65	0.23
Chee and Padiyar (1969)[a]	0.06	0.33	0.15	0.54	51.49	0.11
Martins (1975)[a]	0.10	0.32	0.14	0.57	44.21	0.08
Lenzi et al. (2002)	0.07	0.41	0.18	0.67	78.96	0.00
Chee and Kung (1971)[a]	0.11	0.36	0.20	0.67	73.75	0.15
Meftah and Mossa (2006)	0.18	0.36	0.23	0.76	40.07	0.05
Hoffmans (1998)[d]	0.15	0.32	0.34	0.81	38.65	0.17
Mason and Aruguman (1985)[a]	0.15	0.56	0.32	1.03	86.63	0.15
Gaudio and Marion (2003)	0.07	0.67	0.40	1.14	102.85	0.33
Eggenberger and Müller (1944)[a]	0.35	0.43	0.39	1.17	62.88	0.30
Eggenberger (1943)[a]	0.66	0.38	0.28	1.32	104.77	0.32
Hoffmans and Verhij (1997)	0.33	0.34	0.71	1.38	70.40	0.02
Veronese (1937)[a,e]	0.54	0.50	0.46	1.50	74.90	0.23
Bormann and Julien (1991)	0.38	0.67	0.66	1.71	95.20	0.15
Chee and Yuen (1985)[a]	0.95	0.78	0.80	2.54	108.26	0.00
Bormann (1988)	0.99	0.80	0.85	2.64	112.83	0.03
Damle et al. (1966)[a]	1.08	0.86	0.86	2.80	116.36	0.00
Chee et al. (1972)[a]	0.91	0.80	1.15	2.86	140.74	0.09
D'Agostino and Ferro (2004)	1.00	1.33	1.24	3.57	183.05	0.19
Bhuiyan et al. (2007)	2.25	2.43	2.20	6.87	189.74	0.23

[a]As reported by Bormann and Julien (1991).
[b]Equation a as denoted by Bormann and Julien (1991).
[c]Three-dimensional equation.
[d]Two-dimensional impinging jet equation.
[e]Equation b as denoted by Bormann and Julien (1991).

$$\ln\left(\frac{y_{SE}}{z_U}\right) = -53.649 + 13.548\ln\left(\frac{b_U}{z_U}\right) + 0.481\ln\left[\frac{Q}{b_U z_U\sqrt{g(\Delta-1)d_{90}}}\right] - 11.329\ln\left(\frac{b_U}{B}\right) \quad (8)$$

$$\ln\left(\frac{y_{SE}}{z_W}\right) = 2.618 + 0.831\ln\left[\frac{Q}{b_W z_W\sqrt{g(\Delta-1)d_{90}}}\right] - 1.649\ln\left(\frac{b_W}{B}\right) \quad (9)$$

Eqs. (7)–(9) have square correlation coefficients of 0.978, 0.965, and 0.913, respectively, between observed and predicted scour-depth. Mean square error between observed and predicted values was less than 0.006 m for all equations. Cumulative square error for all weir shapes was 0.040 m^2, cumulative absolute error was 0.74 m, and mean square error was 0.001 m^2. Table 1 shows predicted maximum equilibrium scour depth, and Fig. 8 shows predicted to observed depths. Comparative results for all tests between the original D'Agostino and Ferro (2004) method and the series of proposed dimensionless equations are shown in Fig. 9. As shown in Fig. 9, D'Agostino and Ferro (2004) uniformly overpredicted maximum equilibrium scour depth for the tested structures. Fig. 10 shows the results of Eqs. (7)–(9) as compared with the most accurate approach from Schoklitsch (1932) using cumulative square error as the measure. Mean error between observed and predicted maximum scour depths for proposed methodologies was 10.45%. Schoklitsch (1932) generated a mean error of 37.12%, and D'Agostino and Ferro (2004) produced a mean error of 183.05%.

Discussion

Eqs. (7)–(9) predict laboratory data to a greater degree of accuracy than other approaches; however, the small amount of data available for equation development and associated parameter value ranges place limitations on applicability. Developed equations are sensitive to ranges of parameter values used for regression analyses. If values fall outside of ranges tested, relationships produce extrapolation error and are not reliable design tools. Table 3 shows boundaries of applicability for the dimensionless terms presented in Eq. (6). The dimensionless terms of Eq. (6) are structured to mitigate scaling errors; however, dimensionless scaling theory has not been validated for rock-weir equilibrium scour. Additional field or laboratory information supplementing the existing database would expand the applicability of proposed methodologies.

J. Hydraul. Eng. 2012.138:167-176.

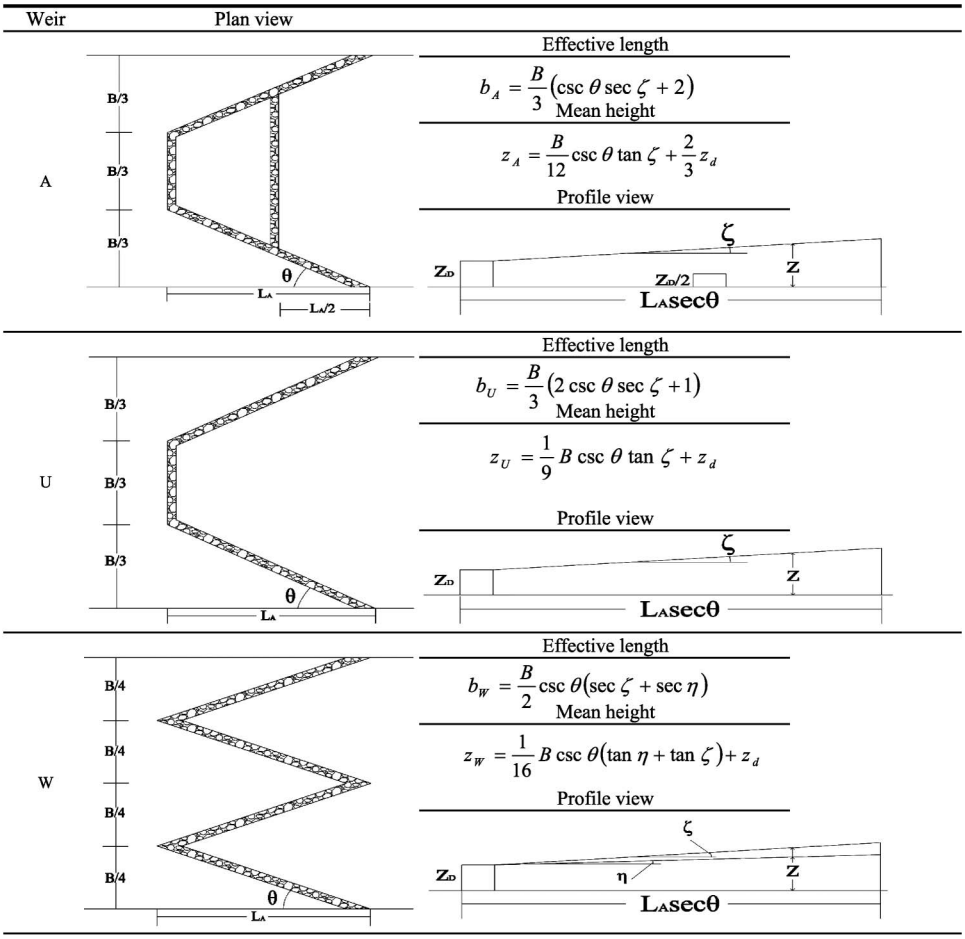

Fig. 7. Weir geometries

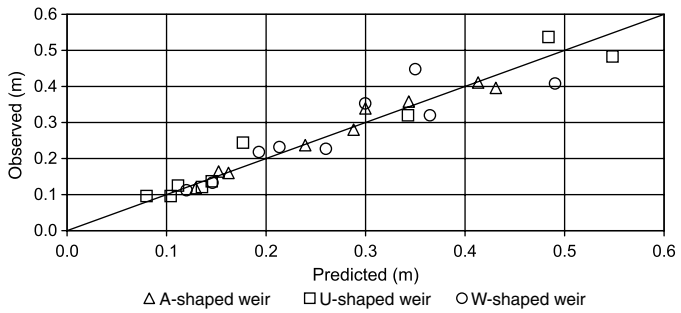

Fig. 8. Observed and predicted equilibrium scour depth

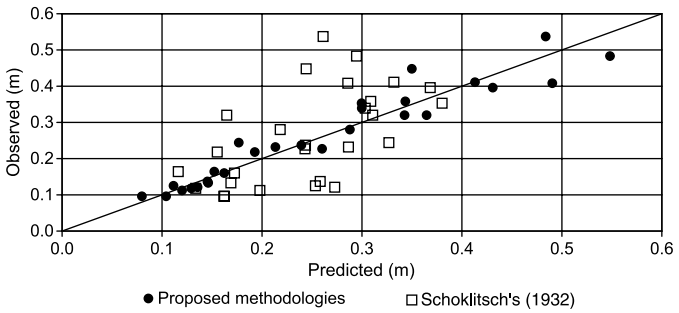

Fig. 10. Eqs. (7)–(9) compared with Schoklitsch (1932)

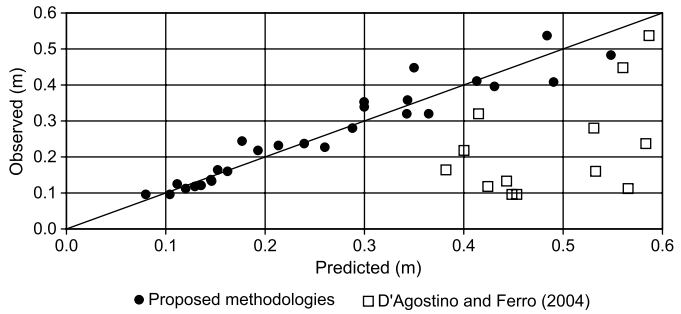

Fig. 9. Eqs. (7)–(9) compared with D'Agostino and Ferro (2004)

Table 3. Tested Parameter Ranges

Shape	$y_{SE\text{-}observed}$ m	π_1	π_2	π_3	π_4	π_5
A						
Maximum	0.411	74.216	2.149	2.894	1.876	1.414
Minimum	0.118	70.069	0.717	0.875	1.435	1.334
U						
Maximum	0.548	102.098	4.113	2.323	1.876	2.042
Minimum	0.064	69.640	0.980	0.527	1.620	1.733
W						
Maximum	0.448	129.348	4.018	1.614	1.876	2.931
Minimum	0.112	120.508	1.015	0.399	1.435	2.231

J. Hydraul. Eng. 2012.138:167-176.

A dimensionless term y_t/H of Eq. (6) was not found to be statistically significant for any weir shape. Large cross correlation was pervasive between y_t/H and the densimetric particle Froude number for all weir shapes, whereby the latter was more statistically significant in all cases. Further testing incorporating parameter values designed to disrupt cross correlations would affect statistical significance within Eq. (6) and potentially alter the format of specific weir equations generated through regression analysis.

Observations of scour geometries led to a series of generalized recommendations for field practitioners. Scour was observed to form at more abrupt changes within the structure, such as the W-shaped weir apexes or at the joining of the A-shaped weir cross bar to the main weir arms. To avoid undermining of the weir, bed armoring or other protective measures may be taken. Structural design of weirs without these abrupt changes, such as a parabolic weir shape, may also mitigate increased scour near the structure. Although maximum scour for the A-shaped weir occurred downstream of the structure cross bar, significant scour formed within the upstream area. Armoring this section with larger grain diameters or riprap may be appropriate to minimize the chance of this scour resulting in unexpected structural failure.

The channel bed was not reset for a configuration between the tested discharges, such that the initial phase of scouring was affected by previous testing, and subsequent tests were serially correlated. The level of this correlation or its influence on equilibrium scour geometry was not determined. Investigation of the effects of initial flat bed versus existing scour geometry conditions is a potential area of focus for future laboratory experiments.

Conclusions

Three-dimensional weirs are gaining popularity as fish habitat improvement, stream rehabilitation, bank stabilization, and grade-control structures. Design criteria for these structures are necessary to prevent failure as a result of downstream scour undermining the structure foundation. A test matrix consisting of A-, U-, and W-shaped weirs with varying discharge, drop height, bed-material size and gradation, slope, arm length, and plan and profile weir angles was designed, tested, and analyzed. Equilibrium scour geometry and maximum scour depth were evaluated for each test. Dimensionless relationships were developed for the maximum equilibrium scour depth, and results were compared with the most accurate method identified in the literature.

Three relationships were developed from the test program database [Eqs. (7)–(9)] to predict maximum scour depth for A-, U-, and W-shaped weirs, respectively. Relationships were determined to be the best predictive approach on the basis of laboratory data and to provide a tool for the prediction of equilibrium scour geometry downstream of rock weirs. Developed equations were compared with the most accurate procedure of Schoklitsch (1932) in prediction of laboratory data and reduced the mean error between observed and predicted values for all tests from 37.12 to 10.45%.

Acknowledgments

The writers sincerely thank the U.S. Bureau of Reclamation for providing funding to perform the research, notably Elaina Holburn and Kent Collins. Jim zumBrennen significantly aided with the statistical portion of the data analysis. Chris Holmquist-Johnson was an integral part in the design of the test matrix and testing procedures. Joseph Mercure, Anthony Meneghetti, and Andrew Fisher collected most of the raw data used in this research.

Notation

The following symbols are used in this paper:

A_1 = morphological jump, defined as the difference between initial and final slope multiplied by the length between structures;
a, b, c, d, e, f, i = equation exponents dependent upon study;
$a_1 \ldots a_6$ = regression coefficients;
B = channel width;
b = weir width;
b_i = effective weir length for weirs $i = \{\mathrm{A}, \mathrm{U}, \mathrm{W}\}$;
d_s = effective grain diameter;
d_{50} = mean sediment diameter;
d_{90} = sediment diameter in which 90% of total is smaller by size;
d_{95} = sediment diameter in which 95% of total is smaller by size;
Fr^* = densimetric particle Froude number;
g = gravitational acceleration;
H = piezometric drop across structure;
H_S = critical specific energy over structure;
H_T = total head drop over structure;
K = coefficient dependent on diffusion and material properties;
Q = discharge;
q = unit discharge over structure;
S_o = bed slope;
u_o = jet velocity over structure;
u_o^* = jet velocity at bed;
V = displaced volume;
y_{SE} = equilibrium scour depth;
y_t = tailwater depth;
y_o = jet thickness entering tailwater;
z = fall height;
z_d = drop height;
z_i = mean weir height above bed for weirs $i = \{\mathrm{A}, \mathrm{U}, \mathrm{W}\}$;
β = jet-impingement angle;
β' = jet-impingement angle at bed;
Δ = specific gravity of material;
ζ = weir outer arm profile angle;
η = W-shaped weir inner arm profile angle;
θ = weir arm plan angle;
ρ = fluid density; and
ρ_S = sediment density.

References

Bhuiyan, F., Hey, R. D., and Wormleaton, P. R. (2007). "Hydraulic evaluation of *w*-weir for river restoration." *J. Hydraul. Eng.*, 133(6), 596–609.

Bormann, N. E. (1988). "Equilibrium local scour depth downstream of grade-control structures." Ph.D. dissertation, Dept. of Civil Engineering, Colorado State Univ., Fort Collins, CO.

Bormann, N. E., and Julien, P. Y. (1991). "Scour downstream of grade-control structures." *J. Hydraul. Eng.*, 117(5), 579–594.

Chee, S. P., and Kung, T. (1971). "Stable profiles of plunge basins." *J Am. Water Resour. Assoc.*, 7(2), 303–308.

Chee, S. P., and Padiyar, P. V. (1969). "Erosion at the base of flip buckets." *Eng. J.*, 52(111), 22–24.

Chee, S. P., Strelchuk, D. L., and Kung, T. (1972). "Configurations of water basin for energy dissipation." *Proc., 86th Annual Congress of Engineering, Institute of Canada*, Saskatoon, Canada.

Chee, S. P., and Yuen, E. M. (1985). "Erosion of unconsolidated gravel beds." *Can. J. Civ. Eng.*, 12(3), 559–566.

J. Hydraul. Eng. 2012.138:167-176.

Comiti, F., D'Agostino, V., Ferro, V., and Lenzi, M. A. (2006). "Fenomeni di erosione localizzata a valle di opere trasversali: Integrazioni tra indagini di campo e di laboratorio." *Quad. Idronomia MT*, 25, 217–225.
D'Agostino, V. (1994). "Indagine sullo scavo a valle di opera trasversali mediante modello fisico a fondo mobile." *Energ. Elettr.*, 71(2), 37–51.
D'Agostino, V., and Ferro, V. (2004). "Scour on alluvial bed downstream of grade-control structures." *J. Hydraul. Eng.*, 130(1), 24–37.
Damle, P. M., Venkatraman, C. P., and Desai, S. C. (1966). "Evaluation of scour below ski jump buckets of spillways." *Proc., Golden Jubilee Symp.*, Vol. 1, Central Water and Power earch Station, Poona, India, 154–163.
Eggenberger, W. (1943). "Die kolkbildung bei einen uberstromen und beider kombination uberstromen-unterstromen." Ph.D. thesis, ETH, Zurich, Switzerland.
Eggenberger, W., and Müller, R. (1944). "Experimentelle und theoretische untersuchungen über das kolkproblem." *Mitteilungen der Versuchsanstalt für Wasserbau*, No. 5, ETH, Zürich, Switzerland.
Fahlbusch, F. E. (1994). "Scour in rock river beds downstream of large dams." *Int. J. Hydropower Dams*, 1(4), 30–32.
Falvey, H. T. (2003). *Hydraulic design of labyrinth weirs*, ASCE, Reston, VA.
Gaudio, R., and Marion, A. (2003). "Time evolution of scouring downstream of bed sills." *J. Hydraul. Res.*, 41(3), 271–284.
Gaudio, R., Marion, A., and Bovolin, V. (2000). "Morphological effects of bed sills in degrading rivers." *J. Hydraul. Res.*, 38(2), 89–96.
Hartung, W. (1959). "Die kolkbildung hinter überstromen wehren im hinblick auf eine beweglich sturzbettgestaltung." *Die Wasser Wirtschaft*, 49(1), 309–313.
Hoffmans, G. J. C. M. (1998). "Jet scour in equilibrium phase." *J. Hydraul. Eng.*, 124(4), 430–437.
Hoffmans, G. J. C. M., and Pilarczyk, K. W. (1995). "Local scour downstream of hydraulic structures." *J. Hydraul. Eng.*, 121(4), 326–340.
Hoffmans, G. J. C. M., and Verhij, H. J. (1997). *Scour manual*, A. A. Balkema, Rotterdam, The Netherlands.
Hopfinger, E. J., Kurniawan, A., Graf, W. H., and Lemmin, U. (2004). "Sediment erosion by görtler vortices: The scour-hole problem." *J. Fluid Mech.*, 520, 327–342.
Jaeger, C. (1939). "Uber die aehnlichkeit bei flussaulichen modellversuchen." *Wasserkraft Wasserwirtsch.*, 34(23/24), 269.
Lenzi, M. A., Marion, A., Comiti, F., and Gaudio, R. (2002). "Local scouring in low and high gradient streams at bed sills." *J. Hydr. Res.*, 40(6), 731–738.
Machado, L. I. (1987). "Discussion on 'Free jet scour below damns and flip buckets,' by P. J. Mason and K. Arumugam." *J. Hydraul. Eng.*, 113(9), 1193–1194.
Martins, R. (1975). "Scouring of rocky river beds and free-jet spillways." *Int. Water Power Dam Constr.*, 27(5), 152–153.
Mason, P. J., and Arumugam, K. (1985). "Free jet scour below dams and flipbuckets." *J. Hydraul. Eng.*, 111(2), 220–235.
Meftah, M. B., and Mossa, M. (2006). "Scour holes downstream of bed sills in low-gradient channels." *J. Hydraul. Res.*, 44(4), 497–509.
Mossa, M. (1998). "Experimental study on the scour downstream of grade-control structures." *Proc., 26th Convengno di Idraulica e Construzioni Idrauliche*, Catanai, Italy, September, 3, 581–594.
Qayoum, A. (1960). "Die gestzmäβigkeit der kolkbildung hinter unterströmten wehren unter spezieller berücksichtigung der gestaltung eines beweglichen sturzbettes." Dissertation, Technischen Hochschule Carolo-Wilhelmina, Braunschweig, Germany.
Reclamation (Bureau of Reclamation). (2007). "River spanning rock structures research." ⟨http://www.usbr.gov/pmts/sediment/kb/spanstructs/index.html⟩ (Oct. 10, 2008).
Schoklitsch, A. (1932). "Kolkbildung unter uberfallstrahlen." *Wasserwirtschaft*, 343.
Scurlock, S. M. (2009). "Equilibrium scour downstream of three-dimensional grade-control structures." M.Sc. thesis, Dept. of Civil and Environmental Engineering, Colorado State Univ., Fort Collins, CO.
Simons, D. B. (1957). "Theory and design of stable channels in alluvial material." Ph.D. thesis, Dept. of Civil Engineering, Colorado State Univ., Fort Collins, CO.
Veronese, A. (1937). "Erosioni di fondo a valle di uno scarico." *Ann. Lav. Pubblici*, 75(9), 717–726.

J. Hydraul. Eng. 2012.138:167-176.